ISBN: 978-3-95450-231-8 ISSN: 2673-5490 doi: 10.18429/JACoW-IPAC2023-THPL049

DESIGN AND COMMISSIONING OF A 200-KV PHOTOCATHODE ELECTRON GUN

Z. Dong*, C. Tan, P. Lv, Z. Dong, Y. Du†, R.Li‡ Department of Engineering Physics, Tsinghua University, Beijing, China

Abstract

Ultrashort electron beams with high brightness are of vital significance in probing nanoscopic dynamics on the pico-to-femtosecond temporal scales. Electron sources are the most critical element in such apparatuses, whose advancements are expected to further improve the resolving capabilities. In this contribution, we report on the development of a DC photocathode electron gun aiming at delivering optimal-quality electron beams for ultrafast electron scattering and photocathode studies. The 200 kV gun features simplicity and adjustability in fabrication and assembling, and is compatible with INFN/DESY/LBNL-type photocathode plugs. The design, fabrication and conditioning processes of the gun are discussed in detail, along with preliminary beam measurement results where nm-scale emittance is demonstrated.

INTRODUCTION

The capture of atomic dynamics in real time is a significant area of interest in academic communities as it can advance our understanding of condensed matter physics, nanomaterials, molecular biology, and other fields. Electron beams, complementing photons, have been widely used to probe nanoscopic dynamics because of their large scattering cross-section, versatility in control and manipulation, and relatively low cost in apparatus construction. Among the various probing techniques, ultrafast electron diffraction (UED) is one of the most productive, in which the electron energy ranges from a few to hundreds of keV from DC photoelectron guns and up to MeV from radio-frequency guns. Thus far, UED apparatuses based on DC photo-guns have made many contributions [1-3]. In such devices, electrons are generated by photoemission from a cathode and accelerated by a static electric field before being focused onto the sample.

The brightness of an electron beam is a critical parameter in ultrafast electron diffraction (UED), where it is defined by the beam density in phase space as $B = I/\pi^2\varepsilon_n^2$, where I is beam current and ε_n is normalized transverse emittance. This parameter primarily determines the resolving power of UED since the reciprocal space resolution $\Delta s = \frac{2\pi}{\lambda_e}\frac{\varepsilon_n}{\sigma_x}$ [4], where λ_e is electron de Broglie wavelength and σ_x is the root-mean-square (rms) beam size at the sample. Thus, maximizing beam brightness from the outset is crucial for achieving high-resolution UED.

* dongzc18@mails.tsinghua.edu.cn
† dych@mail.tsinghua.edu.cn
‡ lirk@tsinghua.edu.cn

At the charge saturation limit, the brightness of a cigar-shaped beam $B_\perp \propto \frac{E_0^{3/2}\sigma_t}{\sigma_r^{1/2}\sigma_{p\perp}^2}$ [5], where E_0 is cathode surface field gradient, and $\sigma_t, \sigma_r, \sigma_{p\perp}$ represent the rms values of beam length, spot size and transverse momentum respectively. Therefore, improving acceleration gradient, reducing photoemission area, and enhancing photocathode performance during gun design are essential strategies for maximizing brightness.

ELECTRON GUN DESIGN

The present work describes the mechanical structure and design considerations of the electron gun. Fig. 1(a) illustrates the cylindrical vacuum chamber of the gun, with various tube extensions for accommodating different components. The top extension holds the high-voltage receptacle that comprises of a ceramic insulation column which complies with the commercial R24 design. The cathode electrode, which features a disk-shaped design with a hemispherical shell, is connected to the negative high voltage through in-vacuum wire. Four ceramic insulating rods mount the cathode electrode to the front panel of the column, providing mechanical support while maintaining electrical isolation. The anode electrode shell, which also serves as a mounting point for in-vacuum focusing and steering coils, is mounted to the front panel. Vacuum angle valves, ion pumps, NEG pumps, and a vacuum gauge are installed in the tube extensions. Two fused-silica viewports on the front panel and optical viewports on the rear panel allow for laser illumination and visual monitoring of the cathode electrode. In a vacuum environment simulation using two 50 L/s ion pumps and eight SAES Capacitorr Z100 NEG pumps, a vacuum pressure of 10^{-9} Pa is achieved. As a result, the gun is compatible with semiconductor photocathodes with high quantum efficiency.

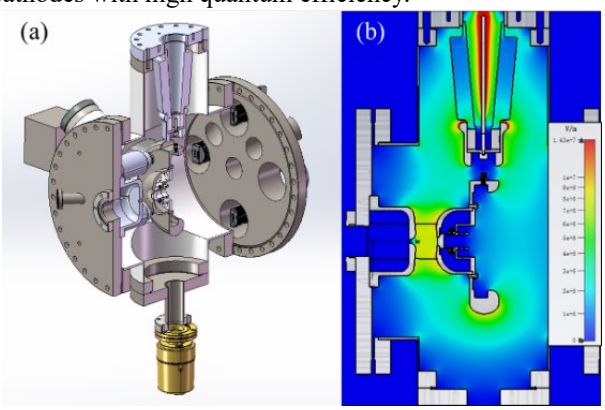

Figure 1: (a) Mechanical structure of the gun. (b) Static electric field simulation at -200 kV voltage.

ISBN: 978-3-95450-231-8 ISSN: 2673-5490 doi: 10.18429/JACoW-IPAC2023-THPL049

A primary consideration during gun design is the optimization of the static electric field, as beam brightness is positively correlated with the accelerating gradient at the cathode surface. However, excessive electric fields can give rise to dark current emission and ultimately electric arcing, compromising high voltage insulation. Thus, a trade-off between accelerating gradient, maximum field on metallic surfaces, and structural compactness must be considered. Figure 1(b) illustrates the results of electric field simulations for the cathode and anode electrodes. A Pierce-type geometry is employed to provide electric focusing during photoemission. The accelerating gap is approximately 25 mm, and the cathode surface gradient is 7.5 MV/m at 200 kV accelerating voltage. To prevent field emission, all other metallic surfaces on the electrodes have different curvatures, such that electric fields do not exceed 12 MV/m. The insulating components bear surface fields less than 8 MV/m and have undergone reliability tests under 225 kV voltage. Particle tracking simulations indicate that the influence of high-order electric fields introduced by the ceramic rods is negligible.

The cathode plug design resembles that of INFN/DESY/LBNL-type photocathode plugs, allowing for research into novel photocathode materials. Additionally, a convex lens with a 12.5-mm focal length lies in the interior of the plug, which, when the cathode substrate is replaced with transparent materials (e.g., quartz), projects a sharp focus of the back-illuminated laser onto the cathode surface. This design provides a minimized photoemission area, and the back-illumination scheme partly depletes electron transverse momenta via photoelectron transportation [6]. Both factors contribute to the elevation of beam brightness.

FABRICATION, ASSEMBLING AND HV CONDITIONING

The metallic components of the gun were fabricated using 316L stainless steel due to its vacuum compatibility and low remanence. After machining and welding, the interior surfaces of the metallic components were rinsed, electrochemically polished, and subjected to high-temperature degassing at 450 ℃ for 48 hours to ensure high vacuum quality. In addition, the electrodes were precisely polished to suppress dark current emission. Ceramic insulating parts were coated with vendor-proprietary coatings. The cathode plug of the gun incorporated a focusing lens and a quartz substrate. While semiconductor photocathodes were on the schedule, a 10-nm copper film cathode was initially used to demonstrate the operation. A peripheral sheet of 100-nm gold film around the substrate ensured electrical conductivity.

The electron gun was assembled in a class-1000 clean room. After installing both electrodes onto the front panel, a camera-based calibration system was used to ensure ~100-μm alignment accuracy. The cathode plug was accommodated in the cathode electrode using spring-loaded screw bolts. The front panel was installed on the column before the high-voltage receptacle was fitted in and connected to the cathode electrode through a short thread of wire, which was shielded by two spherical nuts at both ends. Afterward, other vacuum-related parts, including a 50-L/s ion pump, four Z100 NEG pumps, a vacuum gauge, and vacuum valves, were installed. Laser ports and glass viewports were also positioned on the front and rear panels.

The assembly was subjected to vacuum leak detection using a helium mass spectrometer. After leak detection, the assembly was degassed again at 150 ℃ for 60 hours. After cooling and NEG pump activation, the vacuum pressure reached a level of 2×10^{-8} Pa.

Next, the gun was conditioned at high voltages to eliminate surface field emitters, which reduces the probability of arcing during gun operation. The vacuum pressure inside the chamber and radiation dose rate 0.5 m away from the gun were monitored as indicators of field emission during the conditioning process, as shown in Fig. 2(d). The voltage was rapidly raised to >120 kV and then steadily incremented to ~185 kV. Spikes in vacuum pressure and radiation dose rate marked the moments when field emitters were annihilated through large current emission. After ~36 hours, the conditioning process was suspended at 185 kV for protection and stable operation of the ceramic insulation components.

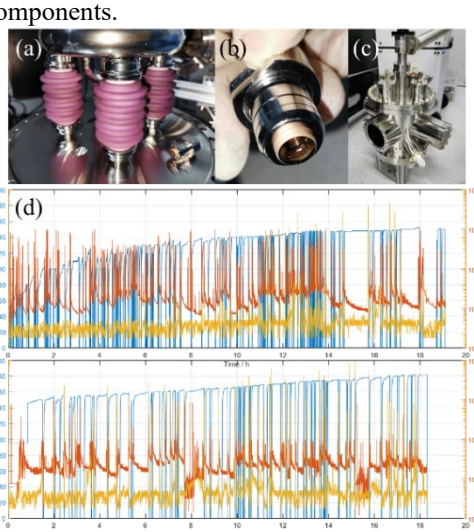

Figure 2: (a) Mounting of electrodes and ceramic rods. (b) Photocathode plug doped with 10 nm copper. (c) Vacuum leak detection. (d) Records of HV conditioning process.

TEST BEAMLINE AND FIRST BEAMS

A test beamline has been designed and constructed to evaluate the performance of an electron gun and to measure the relevant beam parameters. The beamline schematic, as shown in Fig. 3(a), includes an electron gun, a focusing solenoid, several steering magnets, and cube chambers. These chambers contain motor-driven aluminum frames equipped with a Faraday cup, TEM meshes of various pitches, and YAG scintillator screens. In order to prevent charge accumulation, the scintillator screens are doped with 10-nm gold films.

The drive laser is a 266-nm, 20-kHz repetition rate UV laser with 100 ns FWHM pulse duration and 1 μJ maximum pulse energy. An identical cathode plug is installed

ISBN: 978-3-95450-231-8 ISSN: 2673-5490 doi: 10.18429/JACoW-IPAC2023-THPL049

outside the gun to serve as a virtual cathode. For the back-illumination scheme, a Gaussian laser spot of 5 μm rms radius is observed, while for front illumination, the laser spot has a uniform distribution that varies in size from 100 to 300 μm rms by adjusting an aperture and is projected onto the cathode surface at an angle of 40°.

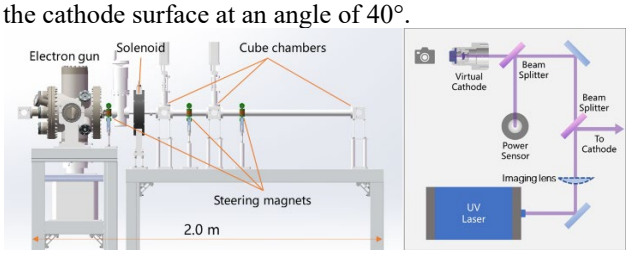

Figure 3: Beamline and drive laser setup.

For front illumination, the quantum efficiency (QE) of the cathode varies from 6×10^{-5} to 8.5×10^{-5} for p-polarization incident laser at 20 to 180 kV; for s-polarization, the QE drops to 65%. Single-shot beam emittance is measured by scanning solenoid focusing. A minimum normalized emittance of ~60 nm·rad is obtained by minimizing aperture size, and the thermal emittance is ~0.52 um·rad/mm. Increasing the beam energy results in a slight increase in emittance, as is shown in Fig. 4.

The generation of nm-scale emittance beams is demonstrated using the back-illumination scheme. Since the emittance is beyond the resolving capability of the solenoid scanning method, a TEM grid is used to perform the measurement [7]. Illustrated in Fig. 5, the 50-time magnified projection of a 1000 mesh/inch TEM grid (with 25 μm pitch and 6 μm bar width) is recorded on a screen 0.3 m downstream of the grid by accumulating 100 shots of electron pulses. The rms angle spread and thus the beam emittance can be determined by fitting the edge spread of the bars. It should be noted that magnification along either direction of the grid is not identical in the presence of astigmatism. As a preliminary result, an approximately 6 nm·rad normalized emittance is recorded for various beam energies, listed in Table 1. It demonstrates the capability of the apparatus to produce an ultra-low emittance beam, but the value is higher than expected. First, the value indicates an upper bound of the single-shot emittance considering laser pointing jitter and mechanical vibration. Also, the actual laser spot on the cathode surface may be larger than estimated on the virtual cathode, as optimal lens focusing in a back-illumination scheme requires excessive installation precision. Further experimental optimization and analysis of the data will be presented in future publications.

Table 1: Preliminary Beam Measurement Results in Back-Illumination Operation Scheme

Parameters	Voltage/kV		
	50	100	150
$\sigma_{x,y}$/μm	18.1, 23.3	15.7, 19.0	14.1, 16.8
$\sigma_{x',y'}$/mrad	0.67, 0.56	0.57, 0.50	0.52, 0.46
$\varepsilon_{nx,ny}$/nm·rad	5.52, 5.91	5.80, 6.22	6.02, 6.27

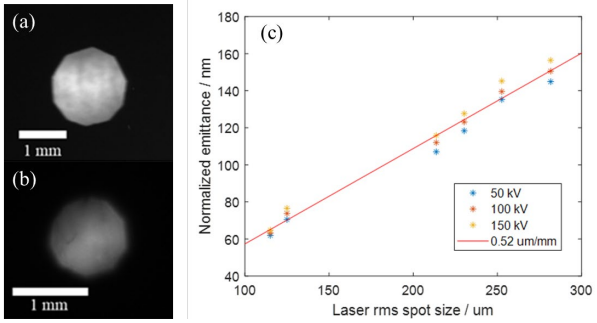

Figure 4: (a) Laser spot on the virtual cathode for front illumination. (b) Corresponding photo-electron beam, recorded by solenoid imaging from cathode surface to scintillator screen. (c) Relationship between beam emittance, laser spot size and beam energy.

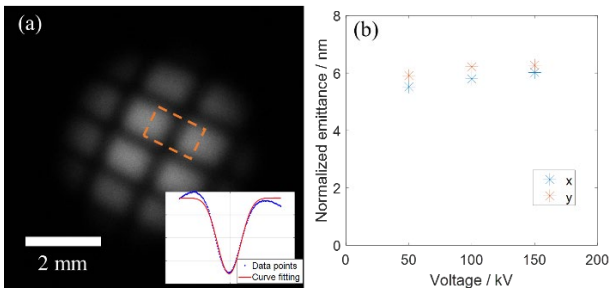

Figure 5: (a) Magnified projection of a TEM grid pattern. Inset: curve fitting of the edge spread of a grid bar. (b) Preliminary emittance measurement results.

CONCLUSION

This paper presents the design, fabrication, and commissioning of a 200-kV photocathode electron gun that is compatible with INFN/DESY/LBNL-type photocathode plugs. Stable operation has been demonstrated up to 180 kV using a 10-nm copper cathode, and several key beam parameters have been measured. In the back-illumination scheme, the apparatus has generated 6-nm emittance beams, confirming its capability to deliver high-brightness electron beams for electron diffraction experiments. Further optimization, such as minimizing the photo-emission area and employing collimation apertures, can be expected to yield sub-nm emittance beams that will enhance both temporal and reciprocal resolutions. The results presented here represent a significant step towards realizing the full potential of this electron gun in various scientific applications.

ACKNOWLEDGEMENT

This work is supported by the Tsinghua University Initiative Scientific Research Program No. 20197050028.

REFERENCE

[1] T. Van Oudheusden *et al.*, "Electron source concept for single-shot sub-100 fs electron diffraction in the 100 keV range", *J. Appl. Phys.*, vol. 102, p. 093501, 2007. doi:10.1063/1.2801027

[2] L. Waldecker *et al.*, "Compact femtosecond electron diffractometer with 100 keV electron bunches approaching the

ISBN: 978-3-95450-231-8 ISSN: 2673-5490 doi: 10.18429/JACoW-IPAC2023-THPL049

single-electron pulse duration limit", *J. Appl. Phys.*, vol. 117, p. 044903, 2015. doi:10.1063/1.4906786

[3] W. H. Li *et al*., "A kiloelectron-volt ultrafast electron micro-diffraction apparatus using low emittance semiconductor photocathodes", *Struct. Dyn.*, vol. 9, p. 024302, 2022. doi:10.1063/4.0000138

[4] S. P. Weathersby *et al.,* "Mega-electron-volt ultrafast electron diffraction at SLAC National Accelerator Laboratory", *Rev. Sci. Instrum.*, vol. 86, p. 073702, 2015. doi:10.1063/1.4926994

[5] D. Filippetto *et al*., "Maximum current density and beam brightness achievable by laser-driven electron sources", *Phys. Rev. ST Accel. Beams*, vol. 17, p. 024201, 2014. doi:10.1103/PhysRevSTAB.17.024201

[6] H. Lee *et al.,* "Intrinsic emittance reduction in transmission mode photocathodes", *Appl. Phys. Lett.*, vol. 108, p. 124105, 2016. doi:10.1063/1.4944790

[7] R. K. Li *et al*., "Nanometer emittance ultralow charge beams from rf photoinjectors", *Phys. Rev. ST Accel. Beams*, vol. 15, p. 090702, 2012.doi:10.1103/PhysRevSTAB.15.090702